REALISTIC 3-DIMENSIONAL EIGENMODAL ANALYSIS OF ELECTROMAGNETIC CAVITIES USING SURFACE IMPEDANCE BOUNDARY CONDITIONS

Hua Guo*, Peter Arbenz†, Computer Science Department, ETH Zurich, Zurich, Switzerland
Benedikt Oswald‡, Paul Scherrer Institute, Villigen, Switzerland

Abstract

The new X-ray Free Electron Laser (SwissFEL) at the Paul Scherrer Institute (PSI) employs, among many other radio frequency elements, a transverse deflecting cavity for beam diagnostics. Since the fabrication process is expensive, an accurate 3-D eigenmodal analysis is indispensable. The software package Femaxx has been developed for solving large scale eigenvalue problems on distributed memory parallel computers. Usually, it is sufficient to assume that the tangential electric field vanishes on the cavity wall (PEC boundary conditions). Of course, in reality, the cavity wall is conductive such that the tangential electrical field on the wall is nonzero. In order to more realistically model the electric field we impose surface impedance boundary conditions (SIBC) arising from the skin effect model. The resulting nonlinear eigenvalue problem is solved with a nonlinear Jacobi–Davidson method. We demonstrate the performance of the method. First, we investigate the fundamental mode of a pillbox cavity. We study resonance, skin depth and quality factor as a function of the cavity wall conductivity. Second, we analyze the transverse deflecting cavity of the SwissFEL to assess the capability of the method for technologically relevant problems.

FORMULATION OF THE PROBLEM

We wish to calculate the resonant frequencies and the corresponding field distribution in a dielectric electromagnetic cavity. The cavity wall Γ is assumed to be of arbitrary shape; there is no aperture or hole in Γ. The surface conductivity σ_s of Γ is large but finite. The interior Ω of the cavity is assumed to be source-free, and is characterized by $(\mu_0\mu_r, \varepsilon_0\varepsilon_r)$. μ_0 and ε_0 are the magnetic permeability and electric permittivity in free space. μ_r and ε_r are relative magnetic permeability and relative electric permittivity, respectively. At microwave frequencies, μ_r and ε_r can be assumed to be non-dispersive.

In the time-harmonic regime, after eliminating the electric field $\mathbf{E}(\mathbf{x})$, the magnetic field $\mathbf{H}(\mathbf{x})$ satisfies

$$\begin{aligned} \nabla \times (\varepsilon_r^{-1} \nabla \times \mathbf{H}(\mathbf{x})) - k_0^2\, \mu_r\, \mathbf{H}(\mathbf{x}) = \mathbf{0}, \quad \mathbf{x} \in \Omega, \\ \nabla \cdot (\mu_r \mathbf{H}(\mathbf{x})) = 0, \quad \mathbf{x} \in \Omega. \end{aligned} \tag{1}$$

Here, $k_0 = \tilde{\omega}\sqrt{\mu_0\varepsilon_0}$ is the *complex* wave number in free space, $\tilde{\omega} = \omega + i\alpha$ is the *complex* angular frequency with ω the angular frequency and α the exponential decay rate.

*hguo@inf.ethz.ch
†arbenz@inf.ethz.ch
‡benedikt.oswald@psi.ch

We use the surface impedance boundary condition (SIBC) on Γ [1]

$$\mathbf{n} \times (\mathbf{n} \times \mathbf{E}(\mathbf{x})) = Z_s\, \mathbf{n} \times \mathbf{H}(\mathbf{x}), \qquad \mathbf{x} \in \Gamma. \tag{2}$$

Here, Z_s is the *complex* surface impedance and $\mathbf{n}$ the surface normal vector pointing outwards.

We employ Z_s based on the theoretical skin effect model [2]

$$Z_s = \frac{1+i}{\sigma_s \delta}, \tag{3}$$

where σ_s is the surface conductivity, and δ is the skin depth. The real part of Z_s is the surface resistivity, i.e.,

$$R_s = \mathrm{Re}(Z_s) = \frac{1}{\sigma_s \delta}. \tag{4}$$

The skin depth δ is [2]

$$\delta = \sqrt{\frac{2}{\omega \mu_0 \mu_r \sigma_s}}. \tag{5}$$

δ depends on the angular frequency ω. Note that the skin effect model is appropriate only if σ_s is large enough such that (according to [2]): (1) the conduction current is given by Ohm's law and the net charge density is zero; (2) the displacement current is negligible in comparison with the current, i.e., $\omega\varepsilon_r\varepsilon_0 \ll \sigma_s$. With the above two assumptions, we consider the conductor is good, and the loss of the cavity is small. In other words, the decay rate $\alpha \ll \omega$, and thus $\omega \approx \tilde{\omega} = k_0 c$, implying that

$$\delta \approx \sqrt{\frac{2}{k_0 c \mu_0 \mu_r \sigma_s}}. \tag{6}$$

The finite element method (FEM) is a suitable method for arbitrary geometrical scales. In order to apply the FEM we use the weak form of Eq (1), see [3],

$$\begin{aligned} &\textit{Find } k_0 \in \mathbb{C} \textit{ and } \mathbf{H} \in V,\ \mathbf{H} \neq \mathbf{0}, \textit{ such that for all} \\ &\mathbf{f} \in V \textit{ and all } q \in W \\ &\int_\Omega \left[\frac{1}{\varepsilon_r} \nabla \times \mathbf{H} \cdot \nabla \times \mathbf{f} - k_0^2 \mu_r \mathbf{H} \cdot \mathbf{f} \right] d\mathbf{x} \\ &\qquad + i k_0 \frac{1}{Z_0} \int_\Gamma (\mathbf{n} \times \mathbf{E}) \cdot \mathbf{f}\, ds = 0, \\ &\int_\Omega \mu_r\, \mathbf{H} \cdot \nabla q\, d\mathbf{x} = 0. \end{aligned} \tag{7}$$

Here, V denotes the functions in $H(\mathbf{curl}; \Omega)$ that satisfy the SIBC boundary conditions and $W = H_0^1(\Omega)$ [1]. $Z_0 = \sqrt{\mu_0/\varepsilon_0}$ is the characteristic impedance of free space.

ISBN 978-3-95450-116-8

Plugging in the SIBC (2), and using (3) and (6), we get

$$\begin{aligned} & ik_0 \frac{1}{Z_0} \int_\Gamma (\mathbf{n} \times \mathbf{E}) \cdot \mathbf{f}\, ds \\ & = ik_0 \frac{Z_s}{Z_0} \int_\Gamma (\mathbf{n} \times \mathbf{H}) \cdot (\mathbf{n} \times \mathbf{f})\, ds \\ & = (i-1) k_0^{\frac{3}{2}} \sqrt{\frac{c\mu_0\mu_r}{2\sigma_s {Z_0}^2}} \int_\Gamma (\mathbf{n} \times \mathbf{H}) \cdot (\mathbf{n} \times \mathbf{f})\, ds. \end{aligned}$$

With this, the weak form (7) becomes

$$\begin{aligned} & \textit{Find } k_0 \in \mathbb{C} \textit{ and } \mathbf{H} \in V,\ \mathbf{H} \neq \mathbf{0}, \textit{ such that for all} \\ & \mathbf{f} \in V \textit{ and all } q \in W \\ & \int_\Omega \left[\frac{1}{\varepsilon_r} \nabla \times \mathbf{H} \cdot \nabla \times \mathbf{f} - k_0^2 \mu_r \mathbf{H} \cdot \mathbf{f} \right] d\mathbf{x} \\ & \quad + (i-1) k_0^{\frac{3}{2}} \sqrt{\frac{c\mu_0\mu_r}{2\sigma_s {Z_0}^2}} \int_\Gamma (\mathbf{n} \times \mathbf{H}) \cdot (\mathbf{n} \times \mathbf{f})\, ds = 0, \\ & \int_\Omega \mu_r\, \mathbf{H} \cdot \nabla q\, d\mathbf{x} = 0. \end{aligned} \tag{8}$$

We discretize problem (8) with the finite element Ritz-Galerkin method [1] employing appropriate finite element subspaces of V and W. To that end we triangulate Ω by tetrahedra. The magnetic vector functions in V are then approximated by Nédélec edge elements, while the scalar functions in W are approximated by Lagrange nodal finite elements [1]. This approach avoids the generation of spurious eigensolutions, and imposing the boundary conditions is straightforward [1].

Let the vector functions $\mathbf{N}_i$, $1 \leq i \leq n$, be the Nédélec basis functions, while the scalar functions N_ℓ, $1 \leq \ell \leq m$, denote the Lagrange basis functions. Eventually, we obtain a constrained complex nonlinear eigenvalue problem

$$T(\lambda)\mathbf{x} = A\mathbf{x} + \lambda^{\frac{3}{2}} R\mathbf{x} - \lambda^2 M\mathbf{x} = \mathbf{0}, \tag{9a}$$

$$C^T \mathbf{x} = \mathbf{0}. \tag{9b}$$

Here $\lambda (= k_0)$ is the eigenvalue and $\mathbf{x}$ is the eigenvector. The matrices A, R, M, and C in (9) have the entries

$$\begin{aligned} a_{ij} &= \int_\Omega \varepsilon_r^{-1} (\nabla \times \mathbf{N}_i) \cdot (\nabla \times \mathbf{N}_j)\, d\mathbf{x}, \\ m_{ij} &= \int_\Omega \mu_r \mathbf{N}_i \cdot \mathbf{N}_j\, d\mathbf{x}, \\ r_{ij} &= (i-1) \int_\Gamma \sqrt{\frac{c\mu_0\mu_r}{2\sigma_s {Z_0}^2}} (\mathbf{n} \times \mathbf{N}_i) \cdot (\mathbf{n} \times \mathbf{N}_j)\, d\mathbf{x} \\ c_{i\ell} &= \int_\Omega \mu_r \mathbf{N}_i(\mathbf{x}) \cdot \nabla N_\ell(\mathbf{x})\, d\mathbf{x}, \\ & \qquad 1 \leq i, j \leq n,\ \ 1 \leq \ell \leq m. \end{aligned}$$

We solve the nonlinear eigenproblem (9a) with the nonlinear Jacobi–Davidson (NLJD) method. The algorithm is taken from Betcke and Voss [4,5]. To impose the divergence-free condition (9b), we construct an appropriate projector to assert that each vector in the NLJD search space is in the null space of C^T, see [6,7].

After having solved (9) the angular frequency ω and the decay rate α are derived from λ. The magnetic field $\mathbf{H}$ is obtained from the calculated eigenvector, the electric field $\mathbf{E}$ by differentiation.

The system's total stored energy U in Ω, and the average power loss P_s in the surface conductor Γ, are computed as [2]

$$\begin{aligned} U &= \frac{\mu_0\mu_r}{2} \int_\Omega |\mathbf{H}|^2\, d\mathbf{x}, \\ P_s &= \frac{R_s}{2} \int_\Gamma |H_t|^2\, d\mathbf{x}. \end{aligned} \tag{10}$$

Here, H_t is the tangential component of the magnetic field on Γ [2]. The systems quality factor can then be defined by

$$Q = \frac{\omega U}{P_s}. \tag{11}$$

NUMERICAL EXPERIMENTS

All simulations have been performed on the Cray XT6 at the Swiss National Supercomputing Centre (CSCS) [8].

Pillbox Cavity

Before simulating the transverse deflecting cavity, we validated the correctness and reliability of our method by means of the elementary pillbox cavity. Let radius and length of the pillbox be $r = 0.05$ m and $h = 0.1$ m, respectively. The mesh contains 306'337 tetrahedra. By using quadratic Nédélec elements, the finite element discretization counts 1'986'080 degrees of freedom (dof). We compute the fundamental TM010 mode with varying surface conductivity σ_s. σ_s is large enough that the two assumptions for a good conductor are satisfied. The results we obtained are listed in Table 1.

Table 1: Numerical analysis for TM010 mode of the pillbox cavity. $f = \frac{\omega}{2\pi}$ is the resonance frequency; δ is the skin depth (5); Q is the quality factor (11).

σ_s (S/m)	f (GHz)	δ (mm)	Q
10^2	2.238100	1.1	30
10^3	2.277208	0.33	99
10^4	2.289538	0.11	316
10^5	2.293434	0.033	1001
$5.8 \cdot 10^7$	2.295160	0.0014	24160
10^{10}	2.295229	0.00011	317255

If σ_s decreases, the field can penetrate into the surface conductor with larger skin depth δ. We understand an increasing δ is equivalent to increasing the volume of the cavity Ω. Therefore, the resonant wavelength increases and the frequency f decreases. Our numerical results clearly show this trend in δ and f.

We also calculated the case of perfect electric conductor (PEC) boundary conditions. Then, $\sigma_s = \infty$

ISBN 978-3-95450-116-8

and $\mathbf{n} \cdot \mathbf{E} = 0$ on Γ. The computed resonance is $f_{\text{pec}} = 2.295234\,\text{GHz}$ [9]. f_{pec} is slightly larger than $2.295229\,\text{GHz}$, where $\sigma_s = 10^{10}\,\text{S/m}$. We observe that if σ_s is $5.8 \cdot 10^7\,\text{S/m}$ (the conductivity of copper), a further increase of σ_s generates almost negligible shift in f, i.e., less than 1 MHz. Therefore, copper is a material well suited for the cavity wall.

The quality factor decreases significantly as σ_s decreases. If σ_s reduces by a factor of 100, then δ_s, R_s and thus P_s increase by a factor of about 10. Therefore, the quality factor reduces by approximately a factor 10.

Transverse Deflecting Cavity

We simulated the 5-cells transverse deflecting cavity. Each cell is a pillbox, and the middle cell is coupled to a rectangular feeding waveguide, see Fig. 1(a). The detailed geometrical parameters of this cavity are given in [10].

We computed the operating TM110 mode with the surface of the conductor being copper, i.e., $\sigma_s = 5.8 \cdot 10^7\,\text{S/m}$. In order to maintain accuracy, we use a mesh containing 872'261 tetrahedra, see Fig. 1(a). By employing quadratic Nédélec elements, the finite element discretization counts 5'726'536 degrees of freedom. 512 cores are used on the Cray XT6.

We obtained the frequency $f = 2.995488\,\text{GHz}$ and the quality factor $Q = 15504$. They match well with the design parameters [10]. The skin depth is $\delta \approx 1.2\,\mu\text{m}$, much smaller than the radius of the cells (58.28 mm). If we replace the SIBC with PEC boundary conditions, the resonance increases slightly from $f = 2.995488\,\text{GHz}$ to $f_{\text{pec}} = 2.995930\,\text{GHz}$. The electrical field distribution $|\mathbf{E}|$ is plotted in Fig. 1(b).

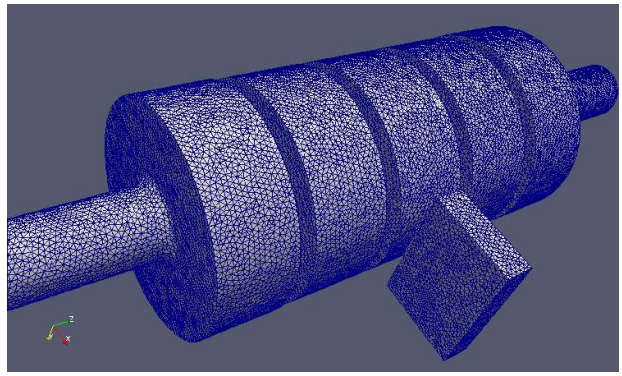

(a)

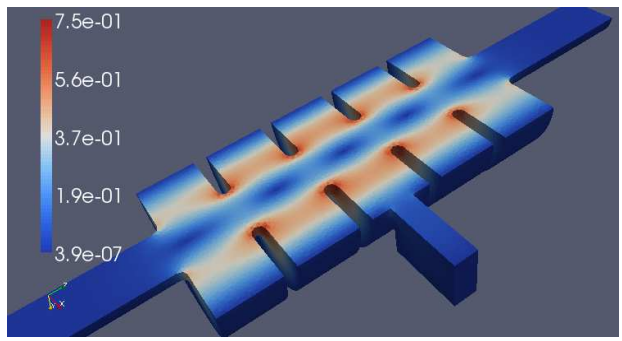

(b)

Figure 1: (a) The geometry and the associated tetrahedral mesh of the 5-cells transverse deflecting cavity. (b) The electric field distribution of the TM110 mode (in half of the domain).

ACKNOWLEDGMENT

It is our pleasure to thank Antonio Falone and Gian-Luca Orlandi (PSI) for sharing thoughts on the transverse deflecting cavity. The work of the first author (H. Guo) was supported in part by grant no. 200021-117978 of the Swiss National Science Foundation.

REFERENCES

[1] J. Jin. *The Finite Element Method in Electromagnetics*. John Wiley, New York, NY, 2nd edition, 2002.

[2] S. Ramo, J. R. Whinnery, and T. Van Duzer. *Fields and Waves in Communication Electronics*. John Wiley, New York, NY, 2nd edition, 1994.

[3] J. Wang and N. Ida. Eigenvalue analysis in electromagnetic cavities using divergence free finite elements. *IEEE Trans. Magn.*, 27(5):3978–3981, 1991.

[4] T. Betcke and H. Voss. A Jacobi–Davidson-type projection method for nonlinear eigenvalue problems. *Future Gener. Comput. Syst.*, 20(3):363–372, 2004.

[5] H. Voss. Iterative projection methods for large-scale nonlinear eigenvalue problems. *Comput. Techn. Rev.*, 1:187–214, 2010.

[6] P. Arbenz, M. Bečka, R. Geus, U. Hetmaniuk, and T. Mengotti. On a parallel multilevel preconditioned Maxwell eigensolver. *Parallel Comput.*, 32(2):157–165, 2006.

[7] R. Geus. *The Jacobi–Davidson algorithm for solving large sparse symmetric eigenvalue problems*. PhD thesis no. 14734, ETH Zurich, 2002.

[8] Homepage of the Swiss National Supercomputing Centre (CSCS): `http://www.cscs.ch/`.

[9] H. Guo, A. Adelmann, A. Falone, C. Kraus, B. Oswald, and P. Arbenz. Computation of electromagnetic modes in the transverse deflecting cavity. In *Proceedings of the First International Particle Accelerator Conference*, pages 1847–1849, May 2010.

[10] M. Pedrozzi. SwissFEL injector conceptual design report. Technical report, Paul Scherrer Institute, 2010.

ISBN 978-3-95450-116-8